

Spatial Orientation of the Antagonist Granisetron in the Ligand-Binding Site of the 5-HT₃ Receptor

Dong Yan and Michael M. White

Department of Pharmacology & Physiology, Drexel University College of Medicine, Philadelphia, Pennsylvania

Received February 10, 2005; accepted May 24, 2005

ABSTRACT

The serotonin type 3 receptor (5-HT₃R) is a member of the cys-loop ligand-gated ion channel (LGIC) superfamily. Like almost all membrane proteins, high-resolution structural data are unavailable for this class of receptors. We have taken advantage of the high degree of homology between LGICs and the acetylcholine binding protein (AChBP) from the freshwater snail *Lymnaea stagnalis*, for which high-resolution structural data are available, to create a structural model for the extracellular (i.e., ligand-binding) domain of the 5-HT₃R and to perform a series of ligand docking experiments to delineate the architecture of the ligand-binding site. Structural models were created using homology modeling with the AChBP as a template. Docking of the antagonist granisetron was carried out using a Lamarckian

genetic algorithm to produce models of ligand-receptor complexes. Two energetically similar conformations of granisetron in the binding site were obtained from the docking simulations. In one model, the indazole ring of granisetron is near Trp90 and the tropane ring is near Arg92; in the other, the orientation is reversed. We used double-mutant cycle analysis to determine which of the two orientations is consistent with experimental data and found that the data are consistent with the model in which the indazole ring of granisetron interacts with Arg92 and the tropane ring interacts with Trp90. The combination of molecular modeling with double-mutant cycle analysis offers a powerful approach for the delineation of the architecture of the ligand-binding site.

The serotonin type 3 receptor (5-HT₃R) is a member of the cys-loop ligand-gated ion channel gene family, which includes the muscle and neuronal nicotinic acetylcholine receptors, the glycine receptor, and the GABA_A receptor (Connolly and Wafford, 2004; Lester et al., 2004). Two different subunits, termed 5-HT_{3A} and 5-HT_{3B}, have been described previously (Reeves and Lummis, 2002). The 5-HT_{3A} subunit forms functional receptors with the appropriate pharmacological properties when expressed in *Xenopus laevis* oocytes or mammalian cells. However, there are some differences between the properties of the expressed homomeric receptors and 5-HT₃Rs in some, but not all, neurons. Perhaps the most significant difference is that the single-channel conductance of the expressed receptors is in the subpicoampere range, whereas that of the receptors in many (but not all) neurons is in the range of 10 to 20 pS (Yang et al., 1992; Hussy et al., 1994). This difference, along with the fact that other members of the cys-loop LGIC family are composed of several different subunits, led to the search and subsequent discov-

ery of an additional 5-HT₃R subunit, now termed the 5-HT_{3B} subunit (Davies et al., 1999; Dubin et al., 1999).

When expressed by itself, the 5-HT_{3B} subunit does not form functional receptors. When the 5-HT_{3B} subunit is coexpressed with the 5-HT_{3A} subunit, the ligand-binding properties of the expressed receptors are identical to those resulting from expression of the 5-HT_{3A} subunit alone (Brady et al., 2001) and of native 5-HT₃Rs. However, whereas homomeric 5-HT_{3A}Rs have single-channel conductances in the subpicoampere range, the heteromeric receptors (i.e., 5-HT_{3A} + 5-HT_{3B} subunits) exhibit single channels with conductances of approximately 15 pS, as seen in many neuronal 5-HT₃Rs (Davies et al., 1999; Dubin et al., 1999). Initial examination of the pattern of expression of the 5-HT_{3B} subunit showed that it was expressed in the same tissues and brain regions as the 5-HT_{3A} subunit, suggesting that all 5-HT₃Rs are heteromeric. However, subsequent expression profiling studies with better spatial resolution (for review, see van Hooft and Yakel, 2003) have cast doubt on the notion that 5-HT₃Rs in the central nervous system are always heteromeric, so the question of subunit composition of “bona fide” 5-HT₃Rs is by no means settled. However, because the ligand-binding profiles of native, homomeric and heteromeric receptors are identical, the structure of the ligand-binding domain of the

This work was supported by a grant from the American Heart Association Pennsylvania-Delaware Affiliate.

Article, publication date, and citation information can be found at <http://molpharm.aspetjournals.org>.
doi:10.1124/mol.105.011957.

ABBREVIATIONS: 5-HT₃R, serotonin type 3 receptor; LGIC, cys-loop ligand-gated ion channel; AChBP, acetylcholine-binding protein; WT, wild type; MDL 72222, 3-tropanyl-3,5-dichlorobenzoate; 5-HT_{3A}R, homomeric 5-HT_{3A} subunit-containing 5-HT₃R.

two types of expressed 5-HT₃Rs and those of native receptors are highly similar. Thus, homomeric 5-HT_{3A}Rs should be an appropriate model for the structure of the ligand-binding domain of native 5-HT₃Rs.

Over the years, structural models for the 5-HT_{3A}R and other members of the ligand-gated ion channel family have been developed, mostly based on the extensive amount of data obtained from studies on the acetylcholine receptor [for review, see Karlin (2002)], and then refined using mutagenesis data from the particular receptor under consideration. At first, these models were not of sufficient resolution to produce detailed models of the architecture of the ligand-binding domains, but the isolation and subsequent determination of the structure at atomic resolution of a homologous acetylcholine-binding protein (AChBP) from the freshwater snail *Lymnaea stagnalis* (Brejc et al., 2001; Smit et al., 2001) has provided a true structure to use as a framework for constructing more realistic models of the extracellular domain of LGICs (Cromer et al., 2002; Le Novère et al., 2002; Maksay et al., 2003; Reeves et al., 2003).

In the case of AChBP-based models of the 5-HT_{3A}R (Maksay et al., 2003; Reeves et al., 2003), ligand-docking simulations produced several orientations of agonists (Reeves et al., 2003) or antagonists (Maksay et al., 2003) in the binding site, and the authors used data obtained from previous mutagenesis studies to evaluate models for consistency with experimental data to select feasible models for receptor-ligand interactions. In this report, rather than using previously obtained data as the determinant of ligand-receptor model feasibility, we use the model itself to guide the design of experiments to test the model employing a variant of double-mutant cycle analysis (Hildago and MacKinnon, 1995). The results of these experiments can then be used to select the ligand-receptor model that is consistent with experimental data, and thus is most likely to be correct.

Materials and Methods

Molecular Biology and Transfection. A full-length cDNA clone corresponding to the 5-HT_{3A(b)} form (Hope et al., 1993) of the receptor was isolated from a neuroblastoma N1E-115 cell line cDNA library as described previously (Yan et al., 1999) and subcloned into vector pCI (Promega, Madison, WI). Site-directed mutagenesis was carried out using the QuickChange system (Stratagene, La Jolla, CA) as described previously (Yan et al., 1999). The nomenclature used to describe mutants is amino acid in wild-type/position/substitution (e.g., W90F). Because the amino terminus of the mature 5-HT_{3A} subunit is unknown, the amino acid numbering system here includes the signal sequence and has the initial methionine as position 1. Please note that the numbering system for the 5-HT_{3A} receptor used in a previous study from this laboratory has changed somewhat so that the W90F and R92A mutations in this study correspond to the W89F and R91A mutations, respectively, in the original study (Yan et al., 1999). Cultures of tsA201 cells, a derivative of the widely-used human embryonic kidney 293 cell line, were maintained in Dulbecco's modified Eagle's medium containing 10% fetal bovine serum, 100 units/ml penicillin, and 100 units/ml streptomycin. Cultures at 30 to 40% confluence were transfected with 20 μ g of receptor cDNA per 100-mm dish using the calcium phosphate technique (Wigler et al., 1979). After 12-h exposure to the DNA/calcium phosphate solution, the medium was replaced with fresh medium, and the cells were allowed to grow for another 24 to 36 h before use. Maximal expression was obtained 36 to 72 h after transfection.

Ligand Binding Assays. Transfected cells were scraped from dishes, washed three times with phosphate-buffered saline, and re-

suspended and homogenized in 2.5 ml of buffer A (154 mM NaCl and 50 mM Tris-HCl, pH 7.4) per 100-mm dish. The homogenate was then used in binding assays or frozen until needed. We observed no change in either ligand affinity or B_{max} values after freezing.

Membranes were incubated for 2 h at 37° in a total volume of 0.5 ml of buffer A containing the appropriate concentrations of antagonist and radioligand ([³H] granisetron; 85 Ci/mmol; PerkinElmer Life and Analytical Sciences, Boston, MA). Binding was terminated by rapid vacuum filtration onto GF/B filters that had been pretreated with 50 mM Tris-HCl, pH 7.4, and 0.2% polyethylenimine, and the filters were washed with 10 ml of ice-cold 50 mM Tris-HCl, pH 7.4, per sample. Nonspecific binding was defined as that binding not displaced by 100 μ M *m*-chlorophenyl biguanide. IC₅₀ values for various antagonists were determined by fitting the data to the equation $\theta = [1 + ([I]/IC_{50})^{n_H}]^{-1}$ using a Levenberg-Marquardt algorithm in a commercially available software package for Macintosh computers (Igor Pro; WaveMetrics, Lake Oswego, OR). θ is the fractional amount of [³H] granisetron bound in the presence of the antagonist at concentration [I] compared with that in the absence of antagonist, IC₅₀ is the concentration of antagonist at which $\theta = 0.5$, and n_H is the apparent Hill coefficient. K_i values were calculated from the IC₅₀ values and the K_d for [³H]granisetron using the Cheng-Prusoff relation (Cheng and Prusoff, 1973): $K_i = IC_{50}/[1 + ([L]/K_d)]$, where [L] is the concentration of [³H]granisetron used to determine the IC₅₀ value in the experiment, and K_d is the dissociation constant for [³H]granisetron. For the Cheng-Prusoff relation to be applicable, the Hill coefficient for the IC₅₀ curve must be equal to 1. In our experiments, all Hill coefficients were not statistically different from unity at a 95% confidence level (data not shown). In this study, all experiments were carried out with a [³H]granisetron concentration equal to its experimentally determined dissociation constant for the particular receptor [WT, 2.1 nM; W90F, 28.6 nM; R92A, 13.6 nM (Table 1)], meaning that the IC₅₀ values were twice the K_i .

Ligands. The structures of the ligands used in this study are shown in Fig. 3. [³H]Granisetron was obtained from PerkinElmer Life and Analytical Sciences, MDL 72222 from Sigma (St. Louis), and ondansetron from GlaxoSmithKline (Uxbridge, Middlesex, UK).

Molecular Modeling. A structural model of the extracellular domain of the mouse 5HT_{3A}R was generated using MODELLER ver. 7.7 (Sali and Blundell, 1993), using the X-ray structure of AChBP as a template [Protein Data Bank code 1I9B (Brejc et al., 2001)]. The sequence alignment between AChBP and 5HT_{3A}R monomers was performed with Align2D from the MODELLER suite, which uses a variable gap opening penalty that depends on the three-dimensional structure of the template. All five subunits were modeled simultaneously to ensure structural integrity between subunits at their interfaces. All polar hydrogens, but not nonpolar hydrogens, were included to allow for main-chain hydrogen bonding. The programs PROCHECK and ProSa2003 were used to evaluate the generated models (Laskowski et al., 1993; Sippl, 1993), and the model that ranked highest by PROCHECK and ProSa2003 was chosen for ligand docking.

Ligand Docking Simulations. 5HT₃R ligands were docked to each binding site in the chosen model using Autodock 3.0 (Morris et al., 1998). Solvation parameters were added to the protein coordinate

TABLE 1
Granisetron orientation in docked models

Docking simulations were carried out using AutoDock as described under *Materials and Methods*. The orientation of granisetron in the binding site of the four clusters with highest affinity was examined to determine which portions of the ligand were near Trp90 and Arg92.

Cluster	Frequency	K_i nM	At Indazole	At Tropane
1	0.6	2.6	Trp90	Arg92
2	0.2	3.4	Trp90	Arg92
3	0.1	4.6	Trp90	Arg92
4	0.1	5.5	Arg92	Trp90

file, and the ligand torsions were defined using the 'Addsol' and 'Autotors' utilities, respectively, in Autodock 3.0. Gasteiger-Marsili charges (Gasteiger and Marsili, 1980), which uses the united atom representation for nonpolar hydrogens, were applied to ligands before docking. The docking was performed with the initial population size set to 100 with 100 independent runs using otherwise default parameters in the standard protocol on a $30 \times 30 \times 40$ -Å grid with spacing of 0.375 Å. The size of the grid gives sufficient freedom for the ligands to be docked in all possible orientations but does not permit them move outside of the binding site. In addition to returning the docked structure, AutoDock also calculates an affinity constant for each ligand-receptor configuration. Images of the receptor with and without docked ligands were produced using the UCSF Chimera package (Pettersen et al., 2004) from the Computer Graphics Laboratory, University of California, San Francisco (supported by National Institutes of Health grant P41-RR01081).

Results

The extracellular domain of the 5-HT_{3A}R was modeled using the known three-dimensional structure of the AChBP from *L. stagnalis* (Brejc et al., 2001) as a template for homology modeling using MODELLER (Fig. 1) (Sali and Blundell, 1993). As with models for the 5-HT_{3A}R reported previously (Maksay et al., 2003; Reeves et al., 2003), each subunit assumes an immunoglobulin-like fold structure (Fig. 1). In the AChBP and, by inference, the other members of the cyst-loop ligand-gated ion channel family, the ligand-binding domain is at the interface between subunits and is made up of a series of six domains (A–F), three from one subunit (A–C), and three from the adjacent subunit (D–F) (Brejc et al., 2001; Celie et al., 2004). Consistent with this notion, studies from several laboratories have identified a number of residues at

or near the 5-HT_{3R} ligand-binding site (Boess et al., 1997; Hope et al., 1999; Yan et al., 1999; Spier and Lummis, 2000; Venkataraman et al., 2002; Yan and White, 2002; Schreiter et al., 2003; Price and Lummis, 2004) that are located in the various binding-site domains in the model.

We used a Lamarckian genetic algorithm (AutoDock; Morris et al., 1998) to create models of antagonist-receptor interactions within the ligand-binding domain using granisetron as the ligand. The models of the 5-HT_{3A}R/granisetron complex produced by this procedure fall into two broad classes (Fig. 2 and Table 1): those with the indazole ring of granisetron near Trp90, and those with the indazole ring near Arg92. Given the various assumptions that underlie the calculations involved in the docking process, using the calculated K_i values to discriminate between models is not appropriate, especially when the K_i values are very close together.

Double-mutant cycle analysis (Carter et al., 1984) can be used to determine whether a particular residue interacts with a particular portion of a ligand. The underlying logic of this approach is that if residue x in the binding site interacts with residue y on the ligand, then the effect of mutating x should depend upon whether residue y in the ligand is changed. An interaction parameter, Ω , is calculated from the K_d or K_i values as $\Omega = (K_{W,L1}/K_{W,L2})/(K_{m,L1}/K_{m,L2})$, where W indicate wild-type receptor, m indicates mutant receptor, and $L1$ and $L2$ indicate the two ligands being compared. An Ω value significantly different from 1 indicates an interaction between the functional group on the ligand and the amino acid on the receptor. Although initially used for analysis of the interaction of peptide toxins with K⁺ channels (Hildago and MacKinnon, 1995), this approach has also been applied

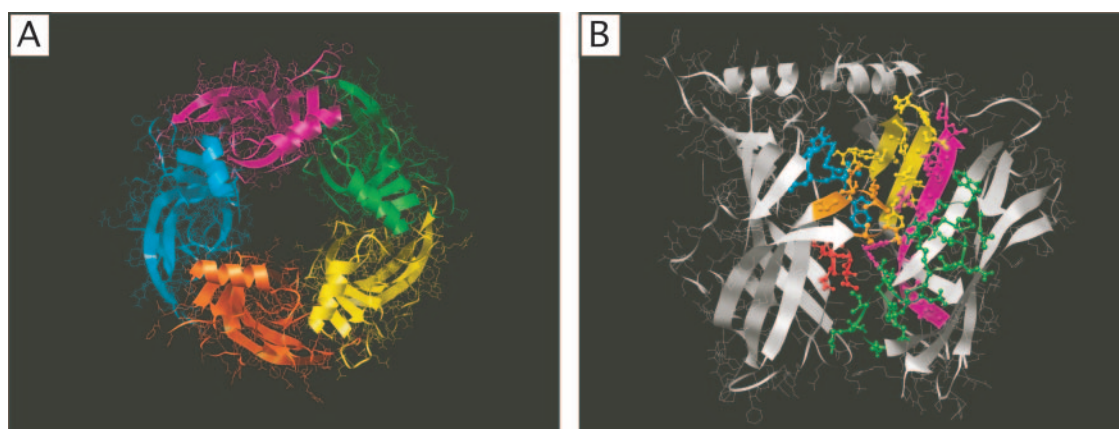


Fig. 1. Structural model of the extracellular domain of the 5HT_{3A}R. A, top view of the pentamer. B, side view of a subunit-subunit interface, with the putative loops in the binding domains (A–F) in color: A, red; B, cyan; C, orange; D, magenta; E, yellow; F, green.

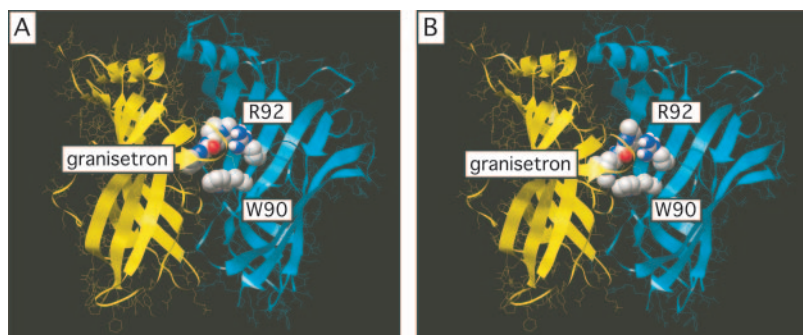


Fig. 2. Granisetron docked in the ligand-binding site. Two representative models of granisetron docked in the ligand-binding domain between two subunits are shown. The 5-HT_{3A}R subunits are shown as ribbon figures with Trp90, Arg92, and granisetron labeled and shown as space-filling structures. In models from clusters 1, 2, and 3 (A), the indazole ring of granisetron is near Trp90 and the tropane ring is near R92, whereas in models from cluster 4 (B), the orientation of granisetron is flipped.

to identify points of contact between acetylcholine receptors and peptide toxins (Malany et al., 2000) or *d*-tubocurarine analogs (Willcockson et al., 2002).

We have used the interaction of three different ligands (granisetron, MDL 72222, and ondansetron; Fig. 3) with wild-type, W90F, and R92A receptors to evaluate the models produced in the docking simulations. These two residues (Trp90 and Arg92) are in loop D of the binding site, and we have shown previously that they play a role in ligand-receptor interactions (Yan et al., 1999). To a crude approximation, MDL 72222 and ondansetron can be thought of as being structural variants of granisetron. In the case of MDL 72222, the indazole ring of granisetron is "mutated" to a chlorobenzoyl ring, whereas in the case of ondansetron, the tropane ring of granisetron is "mutated" to an imidazole ring. Figure 4 shows the inhibition of [³H]granisetron binding to wild-type, W90F, and R92A receptors by MDL 72222. The W90F mutation markedly reduces the affinity for MDL 72222, whereas the R92A mutation slightly increases affinity for the receptor. Table 2 shows the results of the analysis of the interaction of all three ligands with all three receptors. The W90F mutation reduces the affinity for each ligand, whereas the R92A mutation reduces the affinity of granisetron and ondansetron but increases the affinity for MDL 72222.

The combination of three receptors (wild-type, W90F, and

R92A) and three ligands (granisetron, MDL 72222, and ondansetron) gives rise to four double-mutant cycles: a) WT/W90F/granisetron/MDL 72222, b) WT/W90F/granisetron/ondansetron, c) WT/R92A/granisetron/MDL 72222, and d) WT/R92A/granisetron/ondansetron. For each cycle, an interaction parameter, Ω , can be calculated from estimates of the K_d (granisetron) and K_i (MDL 72222 and ondansetron) values of the relevant receptors. Figure 5 shows the four double-mutant cycles that can be constructed, along with the corresponding Ω values. Only two of the cycles have Ω values different from 1.0. The WT/R92A/granisetron/MDL 72222 cycle has an Ω value of 10.8, and the WT/W90F/granisetron/ondansetron cycle has an Ω value of 2.2. When the structures of the three ligands are examined, these data suggest that the indazole ring of granisetron interacts with Arg92 and the tropane ring of granisetron interacts with Trp90. These data can be used to evaluate the ligand-receptor models obtained from the modeling studies, as will be described below.

Discussion

The ultimate goal of molecular modeling is to produce a model that accurately represents the three-dimensional structure of the protein under study. In cases in which actual structural data are missing, homology-based models using

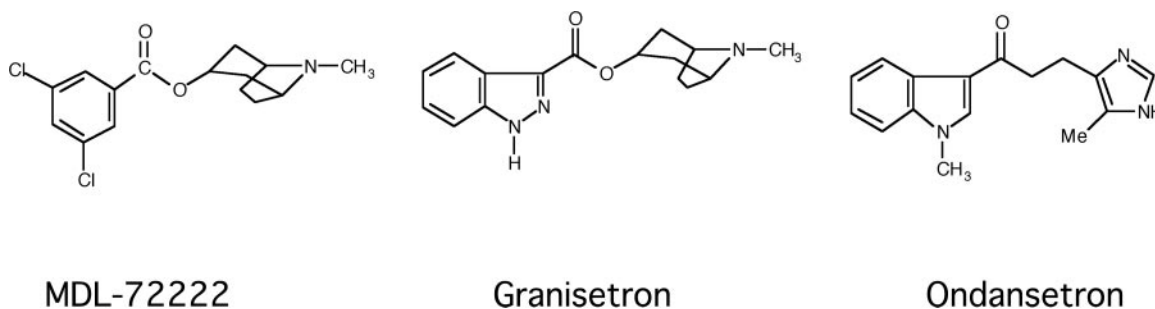


Fig. 3. Structure of ligands used in this study. Note that each ligand can be considered to consist of two "halves": granisetron, indazole/tropane; MDL 72222, chlorobenzoyl/tropane; and ondansetron, indole/imidazole.

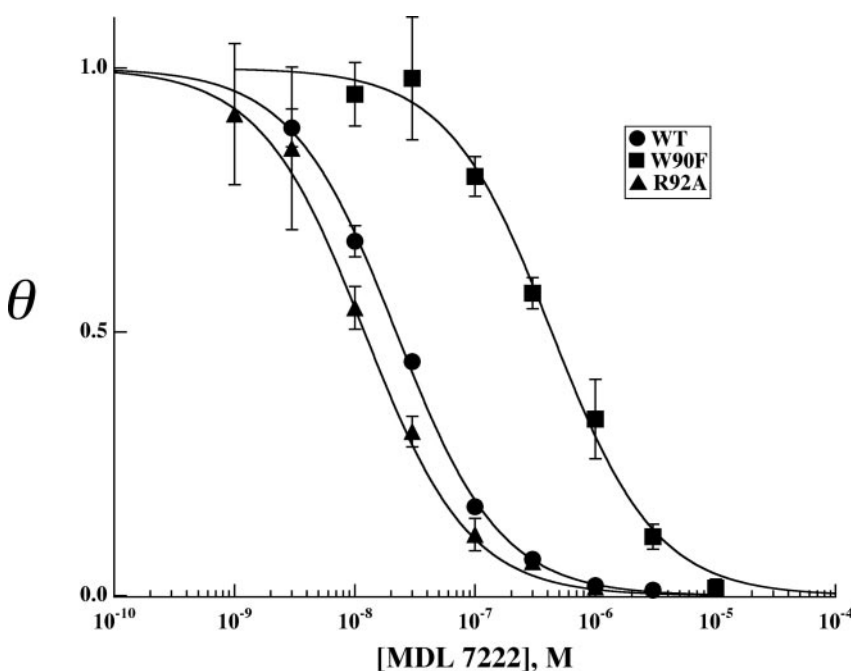


Fig. 4. Effects of W90F and R92A mutations on MDL 72222 affinity. The concentration dependences of inhibition of [³H] granisetron binding by MDL 72222 to wild-type (●), W90F (■), and R92A (▲) 5-HT_{3A}Rs are shown. Each data point represents the mean \pm S.E.M. of three determinations. The solid curves are drawn according to the first equation shown under *Materials and Methods* with IC₅₀ values of 25 nM (wild-type), 500 nM (W90F), and 15 nM (R92A). Note that the W90F mutation decreases MDL 72222 affinity, whereas the R92A mutation increases affinity.

the structures of related proteins have proven to be a useful approach. In the case of cys-loop LGICs, workers have used the structure of the *L. stagnalis* AChBP as a template upon which to build structural models of the extracellular (i.e., ligand-binding) domain of the receptors and have then evaluated the models in light of previously obtained mutagenesis data. Using this approach, two groups have produced models of the 5-HT_{3A}R binding site (Maksay et al., 2003; Reeves et al., 2003). The lack of publicly available Protein Data Bank coordinate files of these other two models precludes a detailed comparison of our model with the other two. The backbone structures of these models are similar to ours, but there are undoubtedly differences in the orientation of side chains within the structures.

The ligand-docking simulations with the antagonist granisetron produced four clusters of docked structures with calculated K_i values in the 2 to 6 nM range, similar to the

experimentally obtained K_i value for wild-type receptors. Three of the models (clusters 1–3; Table 1, Fig. 2A) have granisetron oriented in the binding site such that the indazole ring of granisetron is near Trp90 and the tropane ring is near Arg92, whereas the fourth (cluster 4; Fig. 2B) has the opposite orientation. Maksay et al. (2003) carried out docking simulations with granisetron with the human, mouse, and guinea pig 5-HT_{3A}R. They produced several models of the granisetron-receptor complex, and the lowest energy model was one in which the tropane ring of granisetron was near Trp90 and the indazole ring was closer to Arg92, similar to our cluster 4; other, higher-energy models had the opposite orientation, similar to our clusters 1 to 3. However, the authors did not provide information on either the values of the energies or calculated K_i values, so it is not possible to determine the energy relationships of the different reported conformations.

Given that the calculated K_i values of the four clusters of structures that were produced in this study are very close to each other, choosing one granisetron orientation over the others based solely on calculated K_i values is inappropriate. We chose to test the models using double-mutant cycle analysis. This type of analysis can be used to determine whether or not a particular residue interacts with a particular portion of a ligand (i.e., which parts of a ligand are in close physical proximity to a particular residue). By using three different ligands (granisetron, MDL 72222, and ondansetron), we were able to examine both “halves” of the ligand. The Ω value for the WT/R92A/granisetron/MDL 72222 cycle suggests that the indazole ring of granisetron, but not the tropane ring, interacts with Arg92, whereas the Ω value for the WT/Trp90/granisetron/ondansetron cycle suggests that the tropane ring, but not the indazole ring, interacts with Trp90. Note that the use of the three different ligands provides an internal check for the consistency of the results; i.e., two independent cycles with Ω values >1 lead to the same conclusion regarding the orientation of granisetron in the binding site.

TABLE 2

Affinity of ligands for WT and mutant receptors

Estimates of K_d values for granisetron were determined from saturation binding experiments using [³H]granisetron, and K_i values for MDL 72222 and ondansetron were calculated from experimentally determined IC₅₀ values for the inhibition of [³H]granisetron binding to wild-type or mutant receptors as described under *Materials and Methods*. Each value represents the mean \pm S.E.M. of three separate determinations.

Ligands and Receptors	K_d or K_i nM
Granisetron	
WT	2.3 \pm 0.8
W90F	43.3 \pm 2.1*
R92A	13.6 \pm 0.4*
MDL 72222	
WT	11.1 \pm 0.7
W90F	215.9 \pm 24.9*
R92A	5.9 \pm 0.6*
Ondansetron	
WT	3.0 \pm 1.3
W90F	121.2 \pm 6.2*
R92A	15.6 \pm 2.5*

* Statistically different from wild type at a 95% confidence level using Student's *t* test.

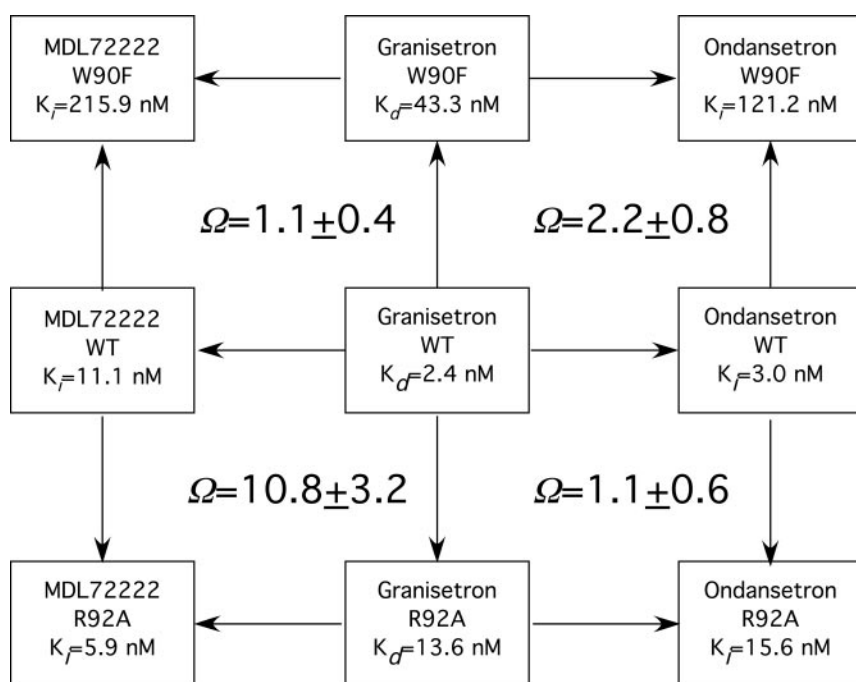


Fig. 5. Double-mutant cycles for WT, W90F, and R92A receptors and granisetron, MDL 72222, and ondansetron. The interaction coefficient, Ω , for all combinations of the three ligands (granisetron, MDL 72222, and ondansetron) with the three receptors (WT, W90F, and R92A) was determined from the K_d or K_i values of each ligand for each receptor. Error estimates were obtained through analysis of propagation of errors (Ku, 1966). The Ω value of 10.8 for the WT/R92A and granisetron/MDL 72222 cycle indicates that R92 interacts with the indazole ring of granisetron, whereas the Ω value of 2.2 for the WT/W90F and granisetron/ondansetron indicates that W90F interacts with the tropane ring of granisetron.

Thus, although the orientation of granisetron in cluster 4 is not as energetically favorable as the others (at least based on calculations), it is the only orientation that is consistent with the double-mutant cycle data, strongly suggesting that this is the actual orientation of granisetron in the ligand-binding site.

The values of Ω from the double-mutant cycle analysis are associated with rather low $\Delta\Delta G$ values (approximately -1.4 kcal/mol for the WT/R92A/granisetron/MDL 72222 cycle, and approximately -0.5 kcal/mol for the WT/Trp90/granisetron/ondansetron cycle), indicating that the interactions are quite weak, because of the type interaction (such as van der Waal's or hydrogen bonds) and/or the distance over which the interaction occurs. Similarly weak interactions were observed in a double-mutant cycle analysis of the interaction of *d*-tubocurarine with the nicotinic acetylcholine receptor (Willcockson et al., 2002).

Reeves et al. (2003) developed a homology-based model of the 5-HT₃R and carried out docking simulations using serotonin as the ligand. Seven different orientations of 5-HT in the binding site were obtained. In the two orientations that they chose as being most likely, the amino group of the indole ring of 5-HT was close to Trp90, but no part of the agonist was near enough to Arg92 to suggest that an interaction formed between Arg92 and the agonist. In other, less-favored orientations, the hydroxyl group of 5-HT was in a pocket containing Arg92, and the side-chain amine was near Trp90. However, none of the models put the indole ring near Arg92. If the indazole ring of granisetron makes interactions similar to those made by the indole ring of 5-HT, then based upon our model, we would expect that the indole of 5-HT would be near Arg92, which none of the agonist-receptor models shows. One possible nontrivial explanation for this is that because of the allosteric nature of ligand-induced channel gating, agonists and antagonists interact with different conformations of the binding site. Thus, one may not expect identical interactions to be observed for agonists and antagonists.

In the present study, we used double-mutant cycle analysis to evaluate various docked orientations of antagonists. Unfortunately, the fact that agonists induce conformational changes in the receptor makes it impossible to obtain accurate estimates of agonist affinity of wild-type and mutant receptors using ligand-binding assays (Colquhoun, 1998). As a result, one cannot evaluate models of agonist-receptor interaction using the experimental approach done here. In the absence of a rigorous method of testing proposed structures of agonist-receptor complexes, extension of our model to agonist-receptor interactions is premature at present.

This study shows the power of double-mutant cycle analysis with small molecule ligands of differing structure to probe ligand-receptor interactions in a way that can map differing portions of the ligand onto specific regions of the receptor. In conjunction with molecular modeling studies, an iterative loop of modeling and experimental testing of models can be created that can accelerate the process of elucidating the three-dimensional architecture of a ligand-binding domain. Inclusion of a wide variety of ligands and mutant receptors should allow the examination of the architecture of the entire ligand-binding domain and thus provide useful information for the design of novel pharmacological agents with both high affinity and high specificity for use as therapeutic agents.

References

- Boess F, Steward L, Steele J, Liu D, Reid J, Glencorse T, and Martin I (1997) Analysis of the ligand binding site of the 5-HT₃ receptor using site directed mutagenesis: Importance of Glutamate 106. *Neuropharmacology* **36**:637–647.
- Brady C, Stanford I, Ali I, Lin L, Williams J, Dubin A, Hope A, and Barnes N (2001) Pharmacological comparison of human homomeric 5-HT_{3A} receptors versus heteromeric 5-HT_{3A/3B} receptors. *Neuropharmacology* **41**:282–284.
- Brejck K, van Dijk WJ, Klaassen RV, Schuurmans M, van Der Oost J, Smit AB, and Sixma TK (2001) Crystal structure of an ACh-binding protein reveals the ligand-binding domain of nicotinic receptors. *Nature (Lond)* **411**:269–276.
- Carter P, Winter G, Wilkinson A, and Fersht A (1984) The use of double mutants to detect structural changes in the active site of tyrosyl-tRNA synthetase (*Bacillus stearothermophilus*). *Cell* **38**:835–840.
- Celie P, van Rossum-Fikkert S, van Dijk W, Brejck K, Smit A, and Sixma T (2004) Nicotine and carbamylcholine binding to nicotinic acetylcholine receptors as studied in AChBP crystal structures. *Neuron* **41**:907–914.
- Cheng Y and Prusoff W (1973) Relationship between inhibition constant (K_i) and the concentration of inhibitor which causes 50 percent inhibition (IC_{50}) of an enzymatic reaction. *Biochem Pharmacol* **22**:3099–3108.
- Colquhoun D (1998) Binding, gating, affinity and efficacy: the interpretation of structure-activity relationships for agonists and the effects of mutating receptors. *Br J Pharmacol* **125**:924–947.
- Connolly C and Wafford K (2004) The cys-loop superfamily of ligand-gated ion channels; The impact of receptor structure on function. *Biochem Soc Trans* **32**:529–534.
- Cromer B, Morton C, and Parker M (2002) Anxiety over GABA_A receptor structure relieved by AChBP. *Trends Biochem Sci* **27**:280–287.
- Davies P, Pistis M, Hanna M, Peters J, Lambert J, Hales T, and Kirkness E (1999) The 5HT_{3B} subunit is a major determinant of serotonin receptor function. *Nature (Lond)* **397**:359–363.
- Dubin A, Huvar R, D'Andrea M, Pyati J, Zhu J, Joy K, Wilson S, Galindo J, Glass C, Luo L, et al. (1999) The pharmacological and functional characteristics of the serotonin 5-HT_{3A} receptor are specifically modified by a 5-HT_{3B} receptor subunit. *J Biol Chem* **274**:30799–30810.
- Gasteiger J and Marsili M (1980) Iterative partial equalization of orbital electronegativity- A rapid access to atomic charges. *Tetrahedron* **36**:3219–3228.
- Hildago P and MacKinnon R (1995) Revealing the architecture of a K⁺ channel pore through mutant cycles with a peptide inhibitor. *Science (Wash DC)* **268**:307–310.
- Hope A, Belelli D, Mair ID, Lambert J, and Peters J (1999) Molecular determinants of (+)-tubocurarine binding at recombinant 5-hydroxytryptamine_{3A} receptor subunits. *Mol Pharmacol* **55**:1037–1043.
- Hope A, Downie D, Sutherland L, Lambert J, Peters J, and Burchell B (1993) Cloning and functional expression of an apparent splice variant of the murine 5-HT₃ receptor A subunit. *Eur J Pharmacol* **245**:187–192.
- Hussy N, Lukas W, and Jones K (1994) Functional properties of a cloned 5-hydroxytryptamine ionotropic receptor subunit: comparison with native mouse receptors. *J Physiol (Lond)* **481**:311–323.
- Karlin A (2002) Emerging structure of the nicotinic acetylcholine receptor. *Nat Rev Neurosci* **3**:102–114.
- Ku H (1966) Notes on the use of propagation of error formulas. *J Res Nat Bur Standards C Eng Instrum* **70**:263–273.
- Laskowski R, MacArthur M, Moss D, and Thornton J (1993) PROCHECK: a program to check the stereochemical quality of protein structures. *J Appl Crystallogr* **26**:283–291.
- Le Novère N, Grutter T, and Changeux J-P (2002) Models of the extracellular domain of the nicotinic receptors and of agonist- and Ca²⁺-binding sites. *Proc Natl Acad Sci USA* **99**:3210–3215.
- Lester H, Dibas M, Dahan D, Leite J, and Dougherty D (2004) Cys-loop receptors: new twists and turns. *Trends Neurosci* **27**:329–336.
- Maksay G, Bukadi Z, and Simonyi M (2003) Binding interactions of antagonists with 5-hydroxytryptamine_{3A} receptor models. *J Recept Signal Transduct Res* **23**:255–270.
- Malany S, Osaka H, Sine S, and Taylor P (2000) Orientation of α -neurotoxin at the subunit interfaces of the nicotinic acetylcholine receptor. *Biochemistry* **39**:15388–15398.
- Morris G, Goodsell DS, Halliday RS, Huey R, Hart W, Belew R, and Olson A (1998) Automated docking using Lamarckian genetic algorithm and an empirical free energy binding free energy function. *J Comp Chem* **19**:1639–1662.
- Pettersen E, Goddard T, Huang C, Couch G, Greenblatt D, Meng E, and Ferrin T (2004) UCSF Chimera: a visualization system for exploratory research and analysis. *J Comput Chem* **25**:1605–1612.
- Price K and Lummis S (2004) The role of tyrosine residues in the extracellular domain of the 5-HT₃ receptor. *J Biol Chem* **279**:23294–23301.
- Reeves D and Lummis S (2002) The molecular basis of the structure and function of the 5-HT₃ receptor: a model ligand-gated ion channel. *Mol Membr Biol* **19**:11–26.
- Reeves D, Sayed M, Chau P-L, Price K, and Lummis S (2003) Prediction of 5-HT₃ receptor agonist-binding residues using homology modeling. *Biophys J* **84**:2338–2344.
- Sali A and Blundell T (1993) Comparative protein modeling by satisfaction of spatial restraints. *J Mol Biol* **234**:779–815.
- Schreier C, Hovius R, Costioli M, Pick H, Kellenberger S, Schild L, and Vogel H (2003) Characterization of the ligand-binding site of the serotonin 5-HT₃ receptor: the role of glutamate residues 97, 224, and 235. *J Biol Chem* **278**:22709–22716.
- Sippl M (1993) Recognition of errors in three-dimensional structures of proteins. *Proteins* **17**:355–362.
- Smit A, Syed N, Schaap D, van Minnen J, Klumperman J, Kits KS, Lodder H, van der Schors R, van Elk R, Sorgedraeger B, et al. (2001) A glia-derived acetylcholine-

binding protein that modulates synaptic transmission. *Nature (Lond)* **411**:261–268.

Spier A and Lummis S (2000) The role of tryptophan residues in the 5-Hydroxytryptamine₃ receptor ligand binding domain. *J Biol Chem* **275**:5620–5625.

van Hooft J and Yakel J (2003) 5-HT₃ receptors in the CNS: 3B or not 3B? *Trends Pharmacol Sci* **24**:157–160.

Venkataraman P, Ventakatachalan S, Joshi P, Muthalagi M, and Schulte M (2002) Identification of critical residues in loop E of the 5-HT_{3AS}R binding site. *BMC Biochem* **3**:15.

Wigler M, Sweet R, Sim G, Wold B, Pellicer A, Lacy E, Maniatis T, Silverstein S, and Axel R (1979) Transformation of mammalian cells with genes from procaryotes and eucaryotes. *Cell* **16**:777–785.

Willcockson I, Hong A, Whisenant R, Edwards J, Wang H, Sarkar H, and Pedersen

S (2002) Orientation of *d*-tubocurarine in the muscle nicotinic acetylcholine receptor-binding site. *J Biol Chem* **277**:42249–42258.

Yan D, Schulte M, Bloom K, and White M (1999) Structural features of the ligand-binding domain of the serotonin 5HT₃ receptor. *J Biol Chem* **274**:5537–5541.

Yan D and White M (2002) Interaction of *d*-tubocurarine analogs with mutant 5-HT₃ receptors. *Neuropharmacology* **43**:367–373.

Yang J, Mathie A, and Hille B (1992) 5-HT₃ receptor channels in dissociated rat superior cervical ganglion neurons. *J Physiol (Lond)* **448**:237–256.

Address correspondence to: Dr. Michael M. White, Department of Pharmacology and Physiology, Drexel University College of Medicine, 245 N. 15th Street, Philadelphia, PA 19102. E-mail: mikewhite@drexel.edu
